Modulation of dayside reconnection during northward interplanetary magnetic field

G. Provan, M. Lester, S. W. H. Cowley, A. Grocott, and S. E. Milan
Department of Physics and Astronomy, University of Leicester, Leicester, UK

B. Hubert
Laboratories de Physique Atmosphèrique et Planètaire, Université de Liège, Liège, Belgium

H. Khan
Research and Scientific Support Department, SCI-SH Division, European Space Agency/European Space Research and Technology Centre, Noordwijk, Netherlands

Received 16 December 2004; revised 3 April 2005; accepted 20 June 2005; published 20 October 2005.

[1] On 17 September 2000 the IMF was directed continuously northward for more than 3 hours. Density fluctuations in the solar wind resulted in quasiperiodic variations in the solar wind dynamic pressure, and correlated fluctuations also occurred in the IMF B_z component. The Northern Hemisphere SuperDARN radars observed bursts of high-latitude high-velocity plasma flow during this northward IMF interval, both when ionospheric signatures consistent with low-latitude merging were observed and when lobe merging was occurring. On average the recurrence period of these flow bursts was ~22 min. During this time the SI-12 spectrographic imager channel on the IMAGE spacecraft observed the dayside proton auroral spot continuously (Frey et al., 2003a). The brightness of the auroral spot varied over time. Here we find a direct correlation between the occurrence of bursts of plasma flow and periodic fluctuations in the brightness of the proton auroral spot. Our results suggest that correlated fluctuations in the solar wind dynamic pressure and IMF B_z component modulated ionospheric precipitation and dayside reconnection, resulting in fluctuations in the brightness of the proton auroral spot and periodic variations in the dayside high-latitude plasma flow.

Citation: Provan, G., M. Lester, S. W. H. Cowley, A. Grocott, S. E. Milan, B. Hubert, and H. Khan (2005), Modulation of dayside reconnection during northward interplanetary magnetic field, *J. Geophys. Res.*, *110*, A10211, doi:10.1029/2004JA010980.

1. Introduction

[2] In recent years several studies have been performed on dayside auroral dynamics and ionospheric convection when the IMF B_z component has been directed northward. These studies have been aided by recent advances in auroral imagers and radar technology, allowing almost global imaging of the auroral regions and of ionospheric high-latitude convection. *Milan et al.* [2000a] studied POLAR UVI observations of the Northern Hemisphere auroral emission during an interval when the interplanetary magnetic field (IMF) had a predominantly positive IMF B_z component, but varying IMF B_y. They reported the existence of a region of luminosity near local noon at latitudes poleward of the dayside auroral oval. This spot corresponded to the ionospheric footprint of the high-latitude reconnection site, and hence the cusp under these conditions. The location of this cusp aurora in latitude and magnetic local time was found to vary in response to changes in the orientation of the IMF. The cusp aurora MLT and the IMF B_y component were especially well correlated, the emission being located in the prenoon or postnoon sectors for $B_y < 0$ nT or $B_y > 0$ nT, respectively.

[3] Subsequently *Frey et al.* [2003a] presented data from the SI-12 imager on the IMAGE spacecraft, showing the occurrence of the dayside proton auroral spot during two intervals of Northward IMF. They reported that the dayside auroral spot was present continuously for many hours. However, the luminosity of the spot varied over time. *Frey et al.* [2003a] interpreted the continuous presence of the proton auroral spot as indicating that the dayside reconnection process is continuous and even quasi-steady. *Frey et al.* [2003a, p. 534] stated that "continuous reconnection operates at a variable rate but never ceases; if the fluctuation is a small fraction of the average then the reconnection is classed as 'quasi-steady.'"

[4] The question of whether dayside reconnection is pulsed or continuous is of fundamental importance to researchers aiming to understand the dayside reconnection process. *Sandholt et al.* [1993, 1998] observed transient optical cusp features associated with intermittent dayside reconnection. *Sandholt et al.* [1994] observed auroral transients and ground magnetic signatures of enhanced convec-

0148-0227/05/2004JA010980$09.00

tion during an interval of negative IMF B_y and B_z. Poleward moving regions of antisunward flow measured by HF radars, suggested to be associated with pulsed dayside reconnection have been reported by *Pinnock et al.* [1995] and *Rodger and Pinnock* [1997]. *Provan et al.* [1998] interpreted pulsed ionospheric flows observed by the SuperDARN radar during a southward IMF interval as the ionospheric signatures of flux transfer events at the dayside magnetopause. *McWilliams et al.* [2000] performed a statistical study on pulsed ionospheric flows observed by the SuperDARN radars, one third of which occurred when the interplanetary magnetic field had a northward component. Recently *Provan et al.* [2005] presented a detailed case study of global convection during an interval of prolonged northward IMF, using the SuperDARN radars. They demonstrated that the relative magnitudes of the IMF B_y and B_z components determined the latitude at which reconnection between the IMF and the Earth's magnetosphere occurred on the magnetopause, and thus whether lobe reconnection only or simultaneous lobe and low-latitude reconnection occurred. Crucially, they concluded that during this case study dayside reconnection was always pulsed.

[5] In this paper we will use the Northern Hemisphere SuperDARN radars to analyze the global convection pattern for one of the intervals discussed by *Frey et al.* [2003a]. Pulsed high-latitude plasma flows are observed during this interval, which we show are directly related to pulsations in the brightness of the dayside proton auroral spot. The combined observations of the dayside proton auroral spot and high-latitude convection demonstrate that high-latitude dayside reconnection may be occurring continuously but the process is certainly not steady, with the signatures of dayside reconnection modulated by pressure pulses occurring in the solar wind which were not discussed by *Frey et al.* [2003a].

2. Instrumentation

[6] The ionospheric convection velocities presented in this study are provided by the Northern Hemisphere SuperDARN radars, part of the international SuperDARN chain of HF radars [*Greenwald et al.*, 1995a]. At present there are 9 SuperDARN radars imaging the high-latitude convection in the Northern Hemisphere. Each radar of the system is frequency agile (8–20 MHz), and routinely measures the line-of-sight (l-o-s) Doppler velocity, the spectral width, and the backscattered power from ionospheric plasma irregularities. The radars each form 16 beams of azimuthal separation 3.24°. Each beam is gated into 75 range bins. In the standard operation (normal resolution) mode used here, each gate has a length of 45 km and the dwell time for each beam is 7 s, giving a full 16 beam scan, covering 52° in azimuth and over 3000 km in range (an area of over 4×10^6 km^2), every 2 min.

[7] In this paper we also present data from the SI-12 images on the IMAGE spacecraft. IMAGE is in a highly elliptical orbit of 1000 km × 45600 km altitude. The FUV instrument consists of three imaging subinstruments and observes the aurora for 5–10 s every 2 min spin period [*Mende et al.*, 2000a, 2000b]. The SI-12 observes Doppler-shifted Lyman-α emission from precipitating protons with energy of several keV. The auroral emission in a particular region depends on the local precipitation characteristics (spectrum and flux) of electrons and protons and the composition of the atmosphere [*Frey et al.*, 2002]. The proton energy fluxes are obtained from the SI-12 count rate using the relationship between the SI-12 signal and NOAA in situ measurements of proton precipitation [*Coumans et al.*, 2002]. The proton energy flux controls the auroral Lyman-α auroral emission [*Hubert et al.*, 2001]. The auroral Lyman-α brightness is then retrieved accounting for the viewing geometry, assuming a 30 keV mean proton energy. Upstream IMF data are provided by the ACE satellite [*Smith et al.*, 1999].

3. Data Presentation

[8] Figure 1 presents the IMF conditions as recorded by the ACE spacecraft on 17 September 2000, from 1600 to 1930 UT. At 1600 UT ACE is positioned upstream of the Earth at GSM position (X, Y, Z) = (231, −33, 21) R_E. We utilized the algorithm of *Lester et al.* [1993] to calculate a 40 ± 7 min. delay between the IMF being observed by the satellite and when it impinges on the dayside magnetopause. Cross correlation between the IMF B_z component, brightness of the proton auroral spot and magnitude of the l-o-s velocity (presented in section 3.4) showed the maximum correlation between these parameters occurred at a delay time of 34 min, which is within the error range of the delay time calculated using the algorithm of *Lester et al.* [1993]. Hence a delay time of 34 min has been added to the timescale of the plots. Figure 1a presents the B_x component (short-dashed line), the B_y component (long-dashed line) and the B_z component (solid line). The IMF B_z component was positive from 16:00 until ~1920 UT. Figure 1b presents the absolute value of the IMF B_y component (dashed) and B_z component (solid). Figure 1c presents the solar wind dynamic pressure. Figures 1d and 1e will be discussed in section 3.3. We have decided to look at two intervals during this period in more detail. During interval A (1620 to 1700 UT) the IMF B_y component was predominantly larger than, or equal to, the IMF B_z component. During interval B (1700 to 1920 UT) the opposite was generally true, with the IMF B_z component being predominantly larger than, or equal to, the IMF B_y component.

[9] Figure 2 presents the f-o-v of the Kapuskasing radar at 1630 UT (Figure 2, top) and 1920 UT (Figure 2, bottom). The plots are in MLAT/MLT coordinates, with 1200 MLT being located at the top of the page. Below we will be presenting l-o-s velocity data from beam 10 of this radar, this beam is marked on the plots with white lines. The plots show that at both 1630 and 1920 UT beam 10 of the Kapuskasing radar is observing the high-latitude noon region in the Northern Hemisphere.

[10] Figure 3 presents the l-o-s velocity data observed in beam 10 of the Kapuskasing radar between 1620 and 1920 UT on 17 September 2000, plotted versus magnetic latitude. The Kapuskasing radar is observing the dayside auroral zone during this time. The plot show color-coded l-o-s velocity as a function of time, where positive values (green and blue) show flows toward the radar, while negative values (yellow and red) show flows away from the radar. A dashed black line separating the two time intervals A and B is marked on the plot. The radar clearly

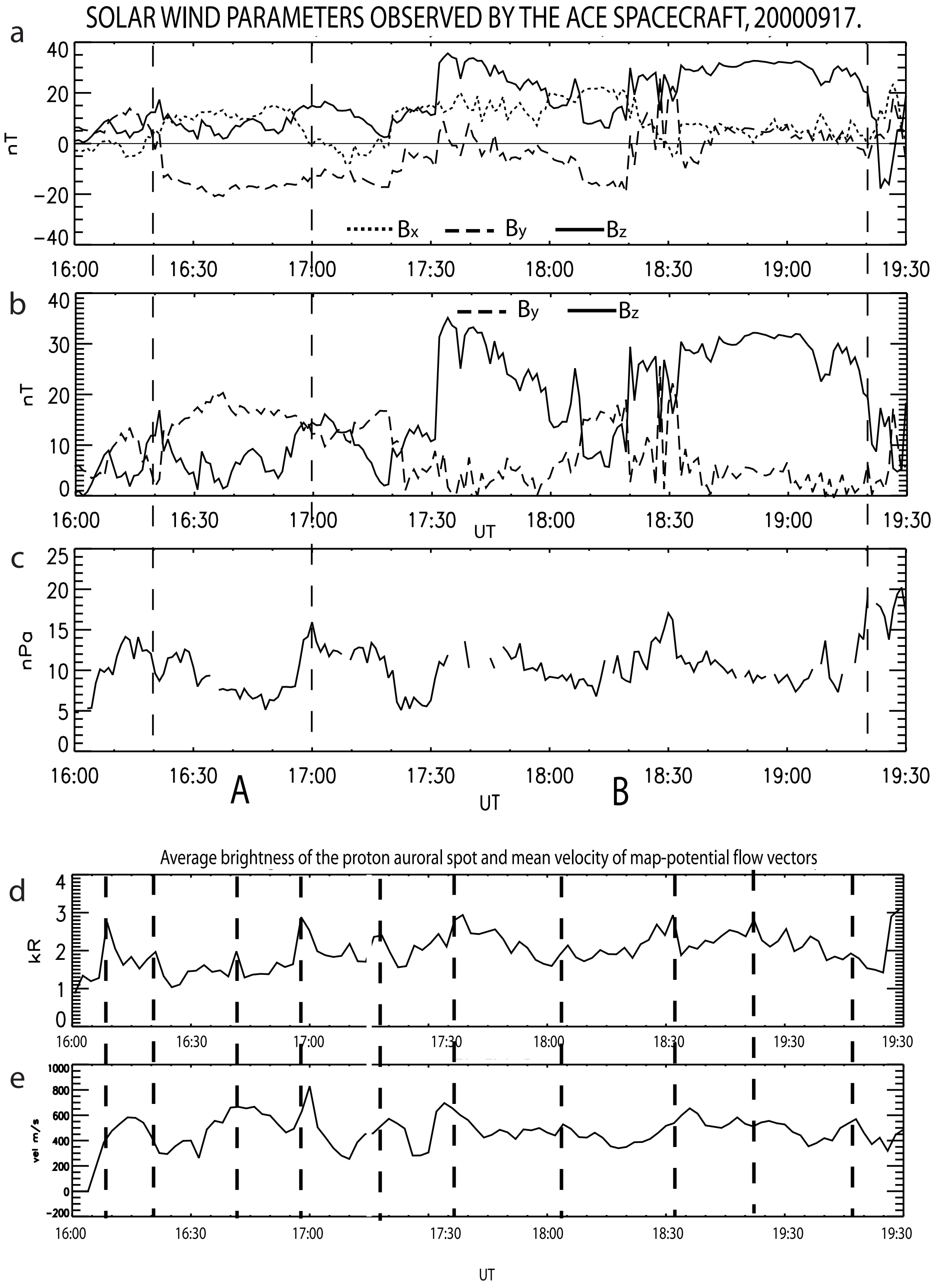

Figure 1. Solar wind parameters observed by the ACE spacecraft, 17 September 2000, 1600 to 1930 UT. A 34 min delay time has been added to the timescale of the plots. (a) IMF B_x component (short-dashed line), the IMF B_y component (long-dashed line), and B_z component (solid line). (b) Absolute value of the IMF B_y component (long-dashed) and the absolute value of the IMF B_z component (solid). (c) Solar wind dynamic pressure for 17 September 2000, 1600 to 1930 UT. Intervals A and B are marked on the plot with dashed black lines. (d) Peak Lyman-α brightness of the proton auroral spot for 17 September 2000 1600 to 1930 UT as observed by the Spectrographic Imager Channel SI-12 on board the IMAGE spacecraft. (e) Average magnitude of the "fitted" map potential flow vectors observed from 1600 to 1930 UT, between 1115 and 1245 MLT above a latitude of 72°.

observes a number of flow bursts of high-velocity transients. Some of these flow bursts have been identified in Figure 3 by red arrows, in order to guide the eye. During interval A two flow bursts are observed, appearing as red stripes in Figure 3, indicating that the l-o-s velocity within each plasma flow burst is directed away from the radar. The transients move to higher latitude with time, with the first flow burst reaching a maximum latitude of 85° at ~1640 UT. During interval B the bursts appear as pulsed blue stripes in Figure 3, indicating that the l-o-s velocity within these transients is directed toward the radar. These flow bursts appear to be moving to lower latitude with time, especially when we consider the backscatter power associated with them (not shown). We will now study the

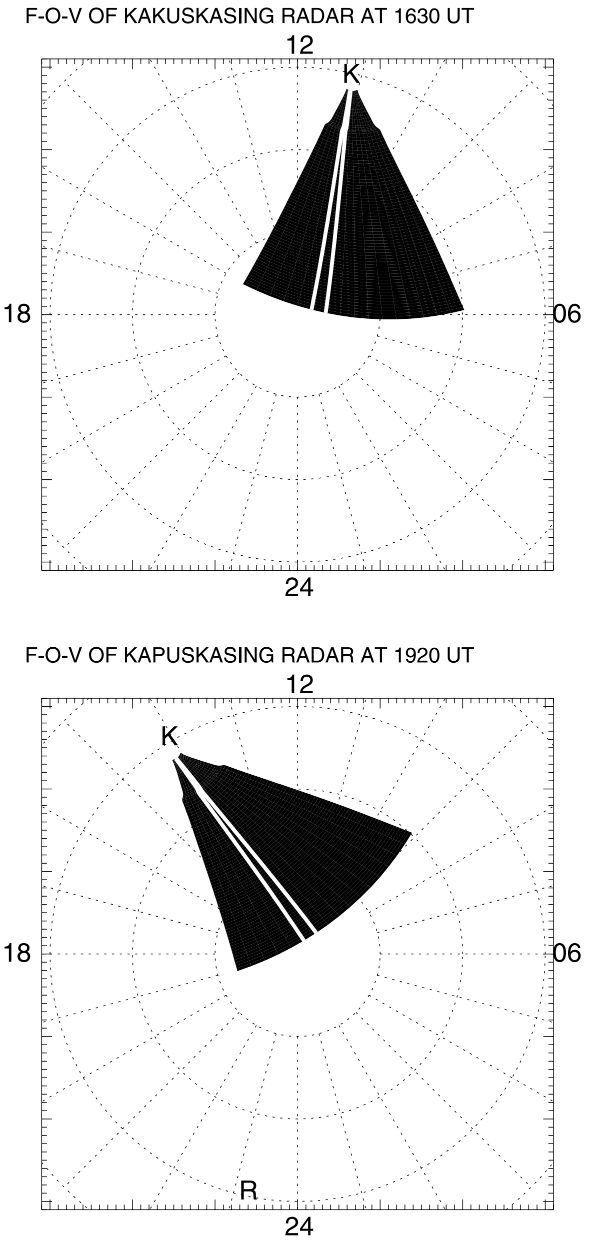

Figure 2. Field-of-view of the Kapuskasing radar at (top) 1630 UT and (bottom) 1920 UT. The plots are in MLAT/MLT coordinates, with 1200 MLT being located at the top. Beam 10 is marked on the plots with open lines.

flow bursts observed during intervals A and B in more detail.

3.1. Interval A

[11] We wish to examine the relationship between the flow bursts observed during interval A and the proton aurora. Figure 4 presents two snapshots of the proton aurora from the spectrographic imager channel SI-12 on board the IMAGE spacecraft as it images the Northern Hemisphere. The images are shown on a geomagnetic grid of latitude and local time, with the noon meridian at the top and dawn to the right. In Figure 4 (left) the auroral images are presented color-coded in intensity. Blue represents the weakest intensity, and red the strongest intensity. All intensities above 1.35 kR are colored red. In Figure 4 (right) the same auroral images are presented in black and white, and with radar data superposed. Snapshots of the proton aurora are presented at two times, at the beginning of the first flow burst at 1633:19 UT (Figure 4, top), and at the end of this first flow burst at 1641:29 UT (Figure 4, bottom). Overlaid on the proton auroral images presented in Figure 4 (right), are the fitted map potential flow vectors and equipotential streamlines for the 2 min intervals 1632–1634 UT (Figure 4, top) and 1640–1642 UT (Figure 4, bottom). These global flow patterns were created by combining l-o-s velocities from all the Northern Hemisphere SuperDARN radars, using the map potential algorithm [*Ruohoniemi and Baker*, 1998]. The technique outputs a number of different vectors. The "fitted" vectors which are presented here are produced by "fitting" the l-o-s velocity vectors to an expansion of the electrostatic potential in spherical harmonics. The l-o-s velocity vectors were obtained from the eight Northern Hemisphere SuperDARN radars available at this time. There is a lack of radar coverage on the local nightside as there is a gap in the global coverage of the SuperDARN radars in this region.

[12] The radars observe two "standard" convection cells, in which the flow rotates in the same direction as ionospheric cells observed under southward IMF conditions, with antisunward flow at high latitude and sunward flow at lower latitude. The dayside convection throat is positioned prenoon and the cusp flow is tilted in an eastward direction. We believe this dawn-dusk asymmetry to be due to the strong negative IMF B_y component during interval A [*Cowley et al.*, 1991]. Simultaneously we can clearly identify the proton auroral oval, within which a spot-like auroral brightening is observed in the noon region. Previous work by, e.g., *Frey et al.* [2003b] has identified such a proton auroral spot lying within the proton oval to be the optical manifestation of the ionospheric footprint of the cusp. *Frey et al.* [2003b] made these observations during intervals of low-latitude merging when the IMF was directed southward. Our observations thus support previous findings by, e.g., *Clauer and Friis-Christensen* [1988], *Freeman et al.* [1993], and *Greenwald et al.* [1995b], suggesting that during intervals of positive IMF B_z and a large IMF B_y, the magnetic shear at the dayside magnetopause is sufficient for reconnection to occur on closed field lines at lower latitudes on the magnetopause, resulting in the excitation of a two-cell convection pattern.

[13] The two flow patterns presented in Figure 4 clearly illustrate how the flow burst observed by the Kapuskasing radar is associated with a strong increase in the plasma flow in the high-latitude cusp region, with much stronger cusp flows being observed at 1640–1642 UT than at 1632–1634 UT. Similar pulsed ionospheric flows (PIFs) have been observed by the SuperDARN radars [*Provan et al.*, 1998], and have been identified as being the ionospheric signatures of flux transfer events occurring at the dayside magnetopause. Figure 4 demonstrates that simultaneously with the increase in the strength of the cusp flow, the proton auroral spot becomes brighter and shifts in longitude. At 1633:19 UT the proton auroral spot is observed in the noon region and has a peak brightness of 1.6 kR. By 1641:29 UT the proton spot has increased in brightness with a peak

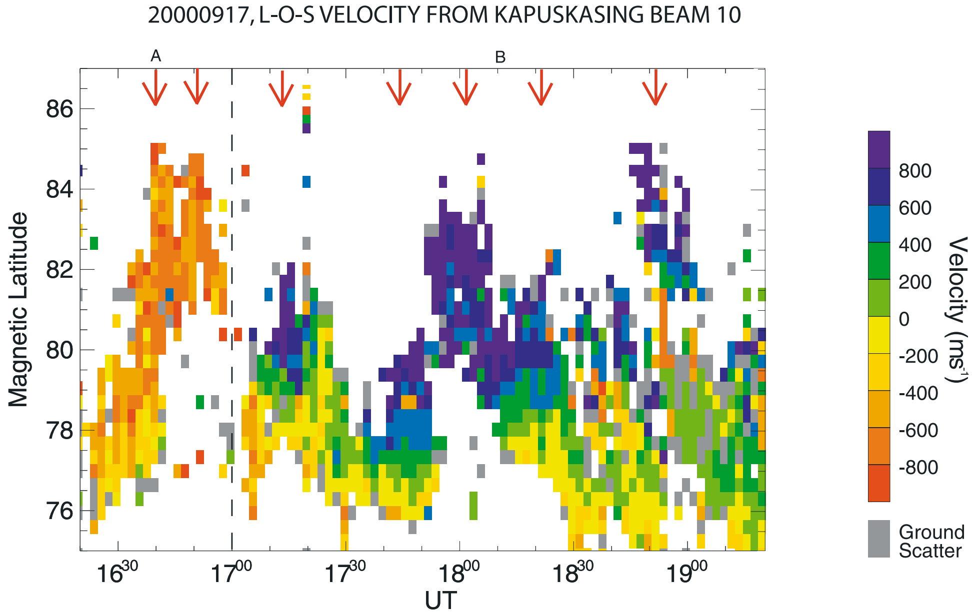

Figure 3. Line-of-sight velocity data observed by beam 10 of the Kapuskasing radar between 1620 and 1920 UT on 17 September 2000, plotted versus magnetic latitude. The Kapuskasing radar is observing the cusp region during this time. The plots shows color-coded l-o-s velocity as a function of time, where positive values (green and blue) show flows toward the radar, while negative values (yellow and red) show flows away from the radar. A dashed black line separating the two time intervals, A and B, is marked on the plot. A selection of flow bursts has been identified with red arrows.

brightness of 2.0 kR, and has shifted to the prenoon region. Interestingly, the proton auroral spot is not necessarily colocated with the strongest cusp flow region. At 1632–1634 UT the cusp flow is observed westward, and slightly poleward, of the proton spot. At 1640–1642 UT the strongest plasma velocities are mainly eastward and poleward of the auroral spot.

[14] During the interval presented in this paper, we noted that the proton auroral spot can be associated with a flow avoidance region. Figure 5 presents four selected proton auroral images observed during interval A at 1621:04, 1651:42, 1655:47 and 1657:50 UT. Overlaid on the plots are the corresponding map potential flow vectors. It can be seen from studying the images that the brightest region of the proton auroral spot is often associated with a lack of radar backscatter and possible flow avoidance, with plasma flow seemingly being diverted around the spot.

3.2. Interval B

[15] During interval B (1700 to 1920 UT) the IMF B_z component is predominantly greater than or equal to the IMF B_y component. Figure 6 shows two snapshots of the proton auroral oval and spot observed by the spectrographic imager channel SI-12 on IMAGE during interval B, and the simultaneous Northern Hemisphere convection patterns, presented in the same format as in Figure 4, but with a slight modification to the color scale. The Kapuskasing radar identified a flow burst at ~1852 UT. Figure 6 (top) presents the proton aurora (1852:12 UT) and the global convection pattern (1852–1854 UT) during the flow burst, and Figure 6 (bottom) presents the proton aurora (1910:35 UT) and the global convection pattern (1910–1912 UT) after the flow burst. The observed global convection patterns are very different from the convection patterns presented in Figure 4. Now the radars observe multicell convection patterns, with "reverse" cells at high latitudes in the dayside sector and the vestiges of "normal" flow cells at lower latitude. The overall flow patterns are typical of flows observed during northward IMF when lobe merging is occurring [e.g., *Heelis et al.*, 1986; *Knipp et al.*, 1991; *Freeman et al.*, 1993; *Huang et al.*, 2000; *Milan et al.*, 2000a].

[16] In both snapshots of the proton aurora, the proton auroral oval and proton spot are clearly observed. The intensity of the proton auroral ovals are enhanced in comparison with the auroral images presented in Figure 4. Indeed the average peak brightness of the proton auroral spot during interval B is 2.7 kR, compared with 2.1 kR during interval A. During interval B the auroral spot has moved poleward of the main auroral oval. *Milan et al.* [2000a] identified the UV auroral spot observed poleward of the UV auroral oval during an interval of northward IMF as the ionospheric footprint of the high-latitude lobe reconnection site. Preliminary results (not presented) demonstrate that during the interval discussed here the proton auroral spot is colocated with enhanced electron precipitation which appears as an elongated arc in the east-west direction, as has previously been observed using high-resolution ground-based optical observations during strongly northward IMF conditions [*Sandholt et al.*, 2000].

[17] As stated above, the Kapuskasing radar observes a flow burst at ~1852 UT. Figure 6 (top) clearly shows enhanced flows within the high-latitude cusp region at this time, compared with the flow pattern observed after the flow burst at 1910:35 UT. These high-velocity plasma flows are observed both within the sunward flow in the cusp

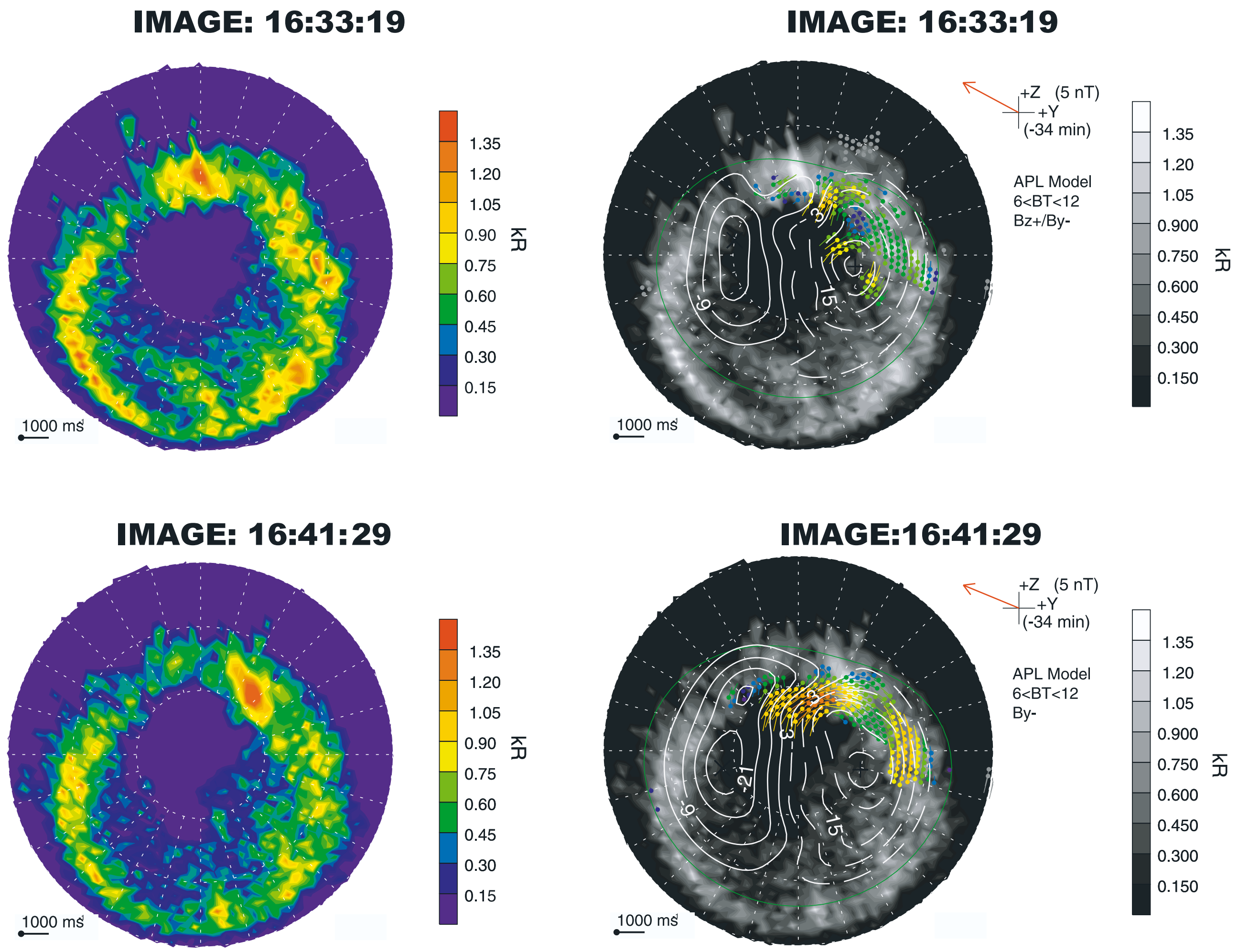

Figure 4. Snapshots of the proton aurora from the spectrographic imager channel SI-12 on IMAGE at (top) 1633:19 UT and (bottom) 1641:29 UT. The images are shown on a geomagnetic grid of latitude and local time, with the noon meridian at the top and dawn to the right. (left) Auroral images color-coded in intensity. The intensity is normalized with blue showing the weakest intensity, and red showing the strongest intensity. (right) Same auroral images presented in black and white, overlaid by the fitted map potential flow vectors and equipotential streamlines for the 2 min intervals, 1632–1634 UT (Figure 4, top) and 1640–1642 UT (Figure 4, bottom).

region, and within the antisunward flow in the postnoon region. Simultaneously, the auroral spot is brighter and larger during the flow burst than after it. Interestingly, the auroral spot again appears to be associated with a lack of radar backscatter.

3.3. Comparison of Proton Aurora and Ionospheric Flows

[18] Figure 7a presents the peak Lyman-α brightness of the proton auroral spot from IMAGE SI-12 for the time interval 1600 to 1930 UT, as presented by *Frey et al.* [2003a]. Figure 7b presents a stack plot of l-o-s velocities observed by beam 8 of the Kapuskasing radar between 1600 and 1930 UT at ranges 44 to 47 (MLAT 77.1° to 78.3°). There is a semiperiodic variation in the brightness of the proton spot and ten peaks in the brightness of the auroral spot, which have been identified by a visual inspection of the data, are marked on the plot with dashed black lines. There is an average interval of ~22 min between the maxima in the brightness of the proton auroral spot. Figure 7 illustrates that there may be a relationship between the dayside high-latitude flow and the brightness of the proton aurora, with peaks in the auroral brightness often occurring simultaneously or almost simultaneously with peaks in the magnitude of the l-o-s velocity (where backscatter is observed). This will be discussed in greater detail below.

3.4. Cross-Correlation Analysis

[19] A cross-correlation analysis of the relationship between the brightness of the proton aurora and l-o-s velocity at Kapuskasing and Goose Bay would clearly be desirable, but this was not possible because of data gaps in the flow observations. Thus we again used the map potential flow patterns. For each map potential convection pattern generated between 1600 and 1930 UT, we averaged the magnitude of all the "fitted" flow vectors observed between 1115 and 1245 MLT. We are interested in comparing how the

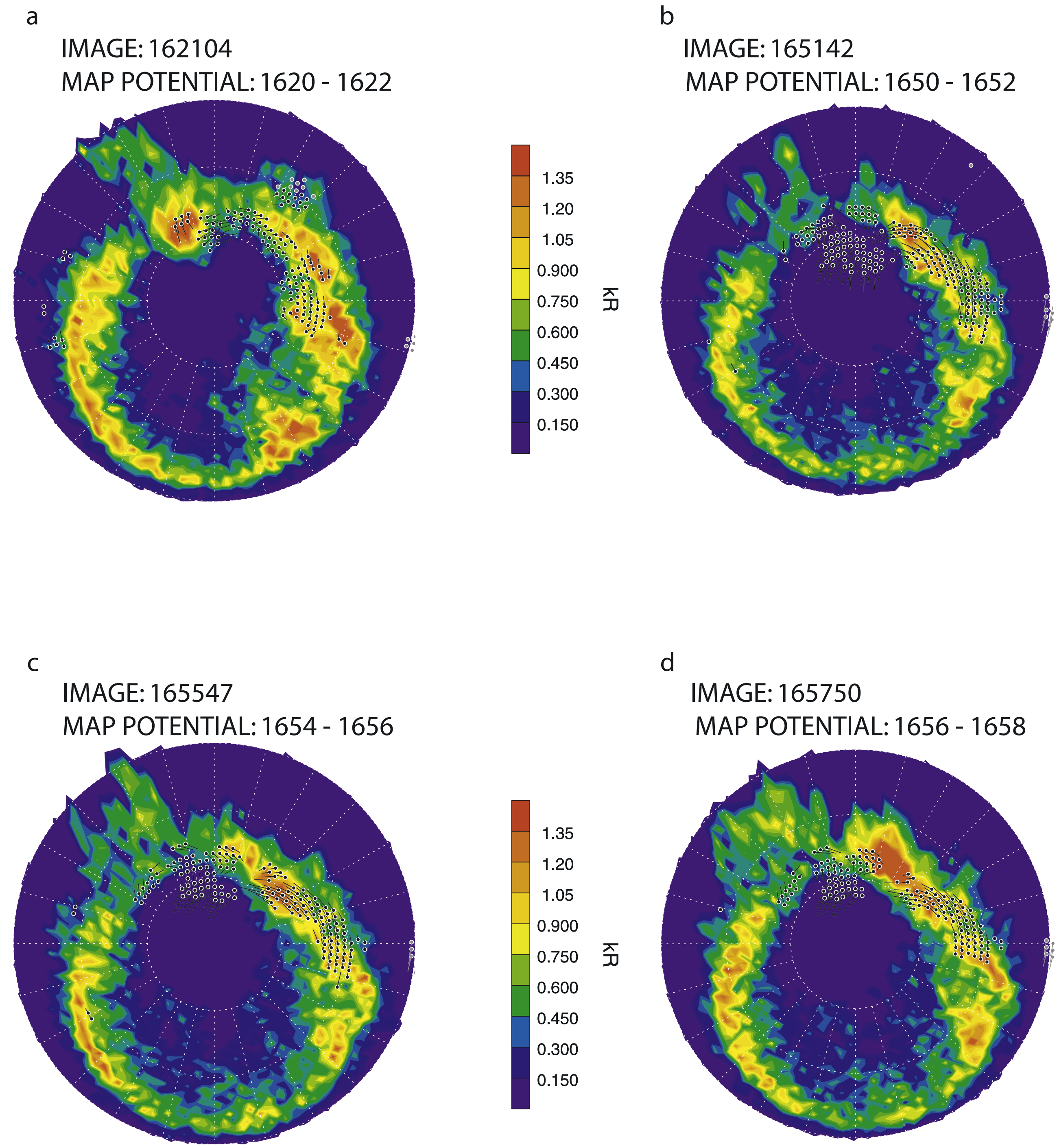

Figure 5. (a) SI-12 proton image at 1621:04 UT and overlaid fitted map potential vectors 1620 to 1622 UT. (b) SI-12 proton image at 1651:42 UT and overlaid fitted map potential flow vectors 1650 to 1652 UT. (c) SI-12 proton image at 1655:47 UT and overlaid fitted map potential vectors at 1654 to 1656 UT. (d) SI-12 proton image at 1657:50 UT and fitted map potential flow vectors 1656–1658 UT.

cusp region flow related to the brightness of the proton auroral spot, thus we only included flow vectors observed above a latitude of 72°, in order to attempt to exclude the return flow observed at lower latitudes. Figure 1d again presents the IMAGE SI-12 detected peak Lyman-α brightness of the proton auroral spot for the time interval 1600 to 1930 UT, as presented in Figure 7. Figure 1e presents the average magnitude of the map potential flow vectors. The magnitude of the flow velocity is predominantly above 400 m s^{-1}. Previous work by *Chisham et al.* [2004], presented observations of strong equatorward flows (~500–800 m s^{-1}) in the noon sector during an interval of prolonged and continuous northward IMF. As can be seen from Figure 1, there is a strong relationship between the peaks in brightness of the proton auroral spot and peaks in the magnitude of the cusp flow velocity. The flow

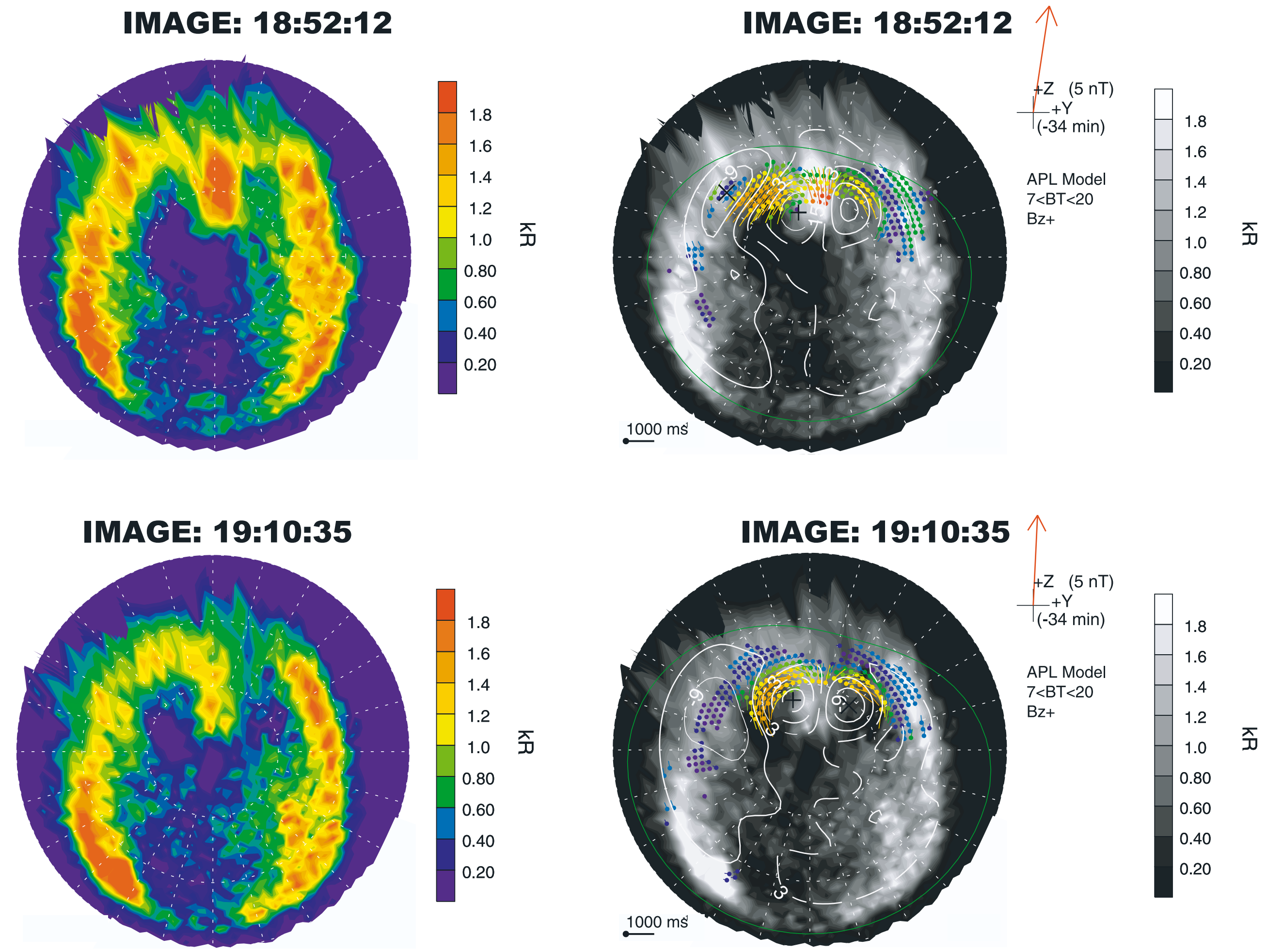

Figure 6. Snapshots of the proton aurora at (top) 1852:12 UT and (bottom) 1910:35 UT presented in the same format as Figure 4. Overlaid on the proton auroral images are the fitted map potential flow vectors and equipotential streamlines for the two minute intervals, 1852–1854 UT (Figure 6, top) and 1910–1912 UT (Figure 6, bottom).

modulations are very strong, with peaks in the flow velocity often having twice the magnitude compared with troughs.

[20] Figure 8 presents six different cross-correlation analyses between the four time series; the peak intensity of the proton auroral spot, the mean magnitude of the map potential flow vectors in the cusp region (already presented in Figure 1), the solar wind dynamic pressure and the IMF B_z component. All the correlation analyses are presented in the same format. For the sake of clarity we confirm that when we state, for example, that the auroral brightness is correlated with respect to the solar wind dynamic pressure, this means that the during the cross correlation the auroral brightness is lagged with respect to the solar wind dynamic pressure. Figure 8a presents the cross correlation analysis of the mean magnitude of the map potential flow vectors in the cusp region with respect to the intensity of the proton auroral spot. Figure 8a (top) presents the auroral brightness, Figure 8a (middle) presents the flow magnitude, and Figure 8a (bottom) presents the cross-correlation coefficient as a function of lag. The dashed lines on Figure 8a (bottom) show the correlation coefficient at which the two time series are correlated at a 99% level of significance. If the two time series are correlated at this level of significance, then there is only a 1% probability that this correlation could have occurred by chance alone such that we conclude that the time series are significantly correlated. At time lags of 0 and ~48 min the correlation coefficient is positive and correlated at the 99% significance level.

[21] Figure 8b presents the cross-correlation analysis of the solar wind dynamic pressure with respect to the IMF B_z component. A 34 min time delay has been added to the timescales of both plots. At a lag of 0 the solar wind dynamic pressure and IMF B_z components are significantly correlated. The correlation coefficient behaves in a periodic manner, reaching a maximum value when the two time series are significantly correlated approximately every 40 min. Studying the solar wind dynamic pressure, it is clear that it too behaves in a cyclical manner, reaching a maximum approximately every 45–50 min.

[22] The auroral intensity is cross-correlated with respect to the solar wind dynamic pressure in Figure 8c, and with respect to the IMF B_z component in Figure 8d. Initial work showed that the maximum correlation between the IMF B_z component and the auroral brightness and ionospheric flow magnitude, and also between the auroral brightness and solar wind dynamic pressure, occurred at a lag of 34 min.

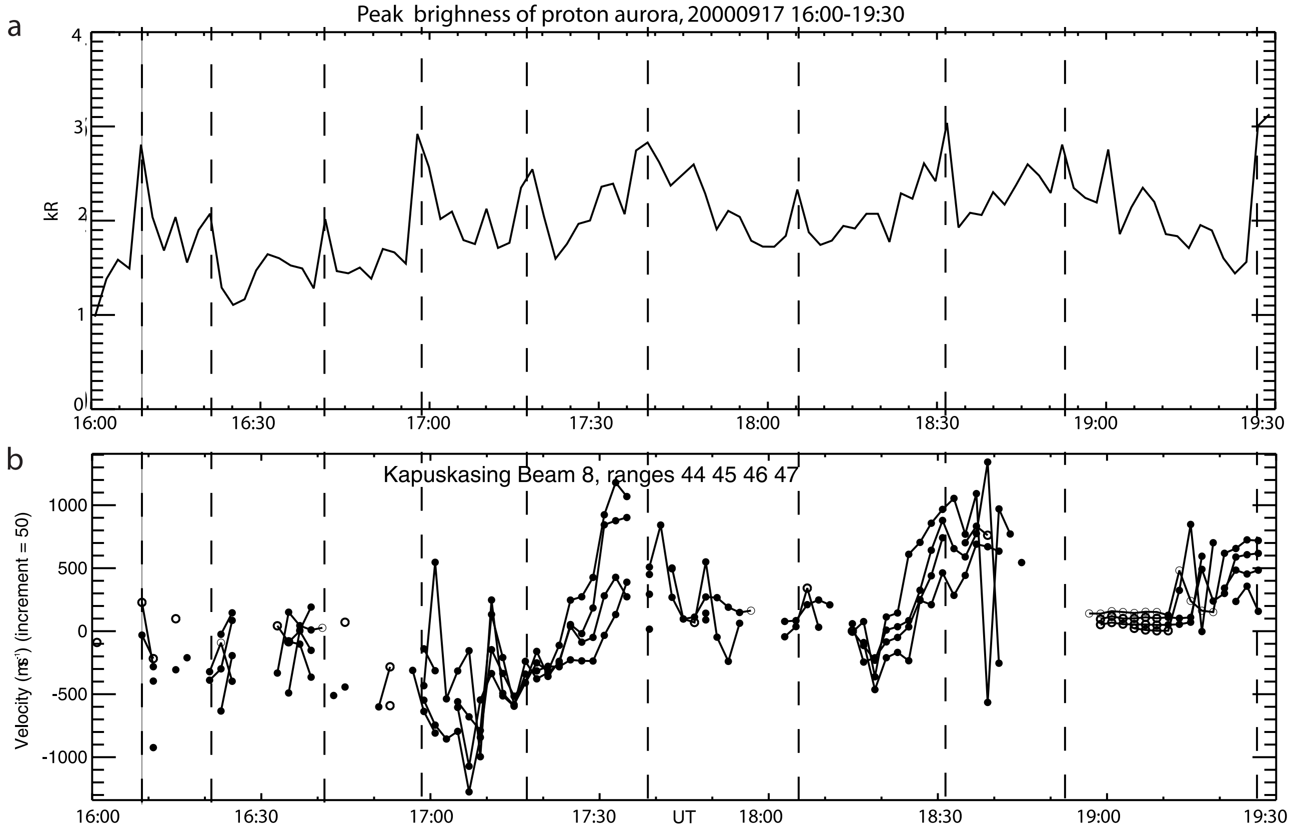

Figure 7. (a) IMAGE SI-12 detected peak Lyman-α brightness of the proton auroral spot for the time interval 1600 to 1930 UT, as presented in Figure 1d. (b) Stack plot of l-o-s velocities observed by beam 8 of the Kapuskasing radar between 1600 and 1930 UT at ranges 44 to 47 (MLAT 77.1 to 78.3).

As already described in section 3, this lag was taken to represent the IMF delay time, and has been added to the timescale of the solar wind dynamic pressure (Figure 8c) and the IMF B_z component (Figure 8d), and is used throughout this analysis. The auroral brightness and solar wind dynamic pressure are correlated at a 99% level of significance at time lags of 0 and $\sim$50 min. At a time lag of zero the correlation coefficient between the auroral brightness and solar wind dynamic pressure is 0.43, while at the same time lag the correlation coefficient between the auroral brightness and IMF B_z is $\sim$0.6. It is interesting to note that the correlation coefficient between the auroral brightness and the IMF B_z component does not have the same cyclical nature as the correlation coefficient between the auroral brightness and solar wind dynamic pressure.

[23] Figure 8e presents the correlation analysis of the magnitude of the ionospheric flow in the cusp region with respect to the IMF B_z component. A time delay of 34 min has been added to the timescale of the IMF B_z component. The correlation coefficient reaches a maximum at time lags of 0 and $\sim$50 min. Figure 8f presents a correlation analysis between the averaged flow magnitude with respect to the solar wind pressure. Again the correlation coefficient peaks at lags 0 min and $\sim$50 min.

[24] The cross-correlation analysis presented above demonstrates that quasiperiodic fluctuations in the solar wind dynamic pressure are correlate to variations occurring in the IMF B_z component. These variations in the dynamic pressure and IMF B_z component are significantly correlated to observed fluctuations in the brightness of the proton aurora and the magnitude of ionospheric flows in the cusp region.

4. Discussion

[25] *Frey et al.* [2003a] studied the proton auroral oval and dayside auroral spot observed on 17 September 2000, and showed that the proton auroral spot is observed continuously for nearly four hours during this day. In this study we have demonstrated that though the spot is continuously present, conditions varied significantly during the interval in a number of aspects. Even though the IMF is directed northward for the entire interval, it is the relative magnitudes of the IMF B_y and B_z components that determine the nature of the dayside reconnection process. During the first part of the interval the IMF B_y component dominated the B_z component. During this time we observed ionospheric convection patterns consistent with low-latitude reconnection occurring at the dayside magnetopause. Previous work by *Provan et al.* [2005] has demonstrated that during a similar interval of weakly northward IMF when a "standard" two-cell convection pattern was observed, lobe and low-latitude reconnection were occurring simultaneously [*Reiff and Burch*, 1985], with a lobe cell observed in the centre of the dusk convection cell. During the second part of the interval the IMF B_z component dominated the B_y component. At this time we observed a global high-latitude

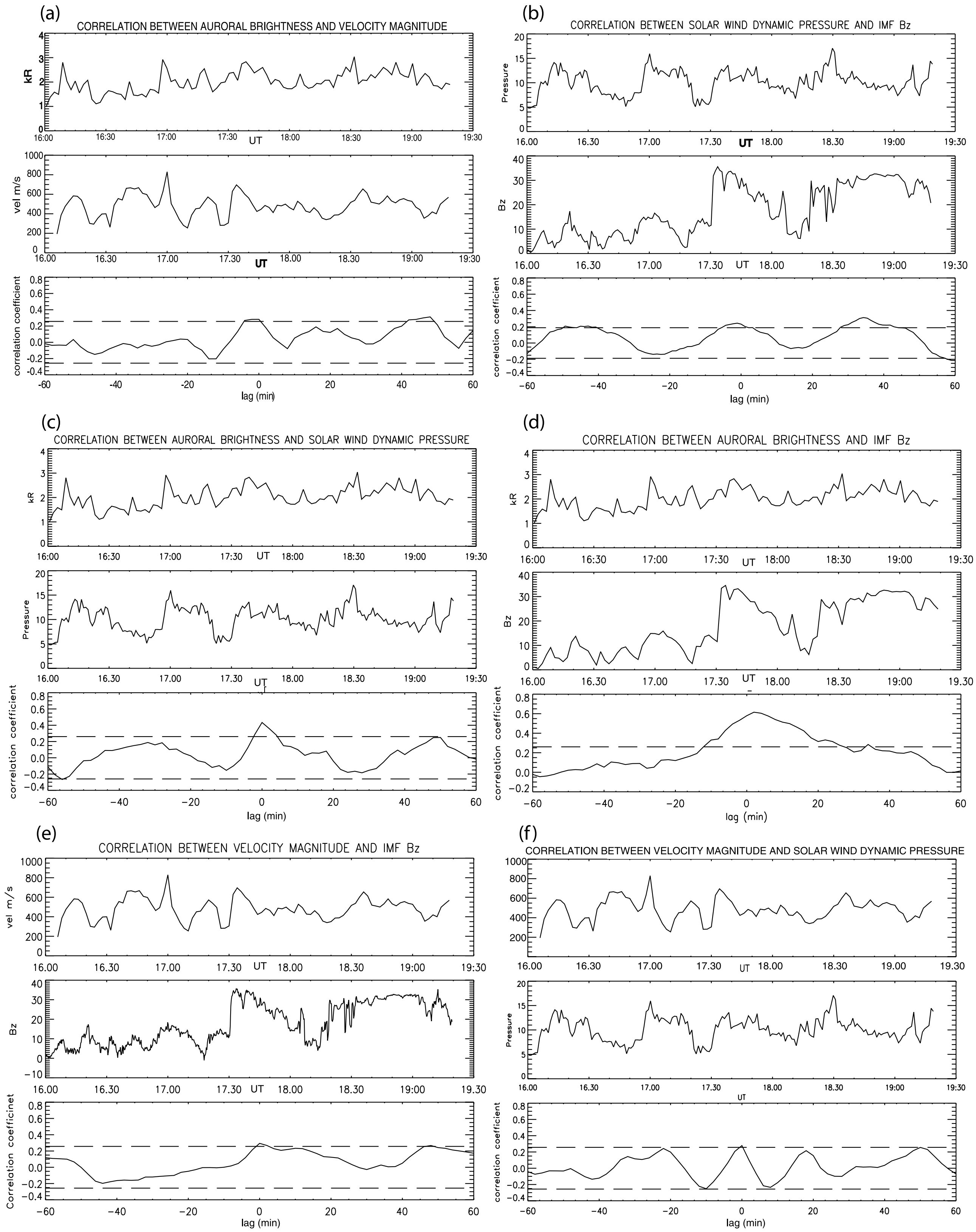
(a)
CORRELATION BETWEEN AURORAL BRIGHTNESS AND VELOCITY MAGNITUDE
kR
vel m/s
UT
correlation coefficient
lag (min)
(b)
CORRELATION BETWEEN SOLAR WIND DYNAMIC PRESSURE AND IMF Bz
Pressure
Bz
UT
correlation coefficient
lag (min)
(c)
CORRELATION BETWEEN AURORAL BRIGHTNESS AND SOLAR WIND DYNAMIC PRESSURE
kR
Pressure
UT
correlation coefficient
lag (min)
(d)
CORRELATION BETWEEN AURORAL BRIGHTNESS AND IMF Bz
kR
Bz
UT
correlation coefficient
lag (min)
(e)
CORRELATION BETWEEN VELOCITY MAGNITUDE AND IMF Bz
vel m/s
Bz
UT
Correlation coefficinet
lag (min)
(f)
CORRELATION BETWEEN VELOCITY MAGNITUDE AND SOLAR WIND DYNAMIC PRESSURE
vel m/s
Pressure
UT
correlation coefficient
lag (min)

Figure 8

convection pattern consistent with lobe merging occurring at the dayside magnetopause.

[26] The proton auroral oval and dayside auroral spot were observed during the entire interval. When low-latitude merging was observed the proton auroral spot was observed within the auroral oval at a location we take to be the footprint of the ionospheric cusp. When high-latitude merging was observed the auroral spot was observed poleward of the auroral oval at the footprint of the high-latitude reconnection site and cusp [*Milan et al.*, 2000a; *Fuselier et al.*, 2002]. The intensity of the proton auroral oval and spot was much enhanced during the interval when the high-latitude lobe merging occurred.

[27] We have demonstrated that the intensity of the proton auroral spot varies with time both during intervals of lobe merging and during intervals of low-latitude merging, with an average periodicity of ~22 min. The variation in the intensity of the proton auroral spot is directly correlated to variations in the magnitude of the flow velocity as observed by the SuperDARN radars, with the brightest proton auroral spot being observed when flow bursts are observed in the cusp region by the SuperDARN radars. Ionospheric flow bursts have previously been identified as the ionospheric signatures of pulsed dayside reconnection occurring during intervals of low-latitude merging when the IMF points southward [e.g., *Pinnock et al.*, 1995; *Provan et al.*, 1998]. During the case study presented by *Provan et al.* [1998], the SuperDARN HF radar at lower latitudes observed the flow bursts as poleward moving region of enhanced convection flows. At higher latitudes the pulsed flows were observed as poleward moving regions of backscatter. Such poleward moving regions of backscatter, also identified by *Milan et al.* [2000b] as a convection response to transient reconnection, are consistent with the observations made here.

[28] During interval A the flow bursts are observed poleward of the proton auroral spot, suggesting that these flow bursts may be consistent with the high-latitude flux transfer events recently reported by *Farrugia et al.* [2004] and *Thompson et al.* [2004]. *Farrugia et al.* [2004] reported observing pulsed flows poleward of the convection reversal boundary during an interval of negative IMF B_z, and suggested that the high-latitude boundary layer downstream of the cusp might be an active site of momentum transfer. *Thompson et al.* [2004] reported observing high-latitude flux transfer events in the northern dayside lobe poleward of the cusp during an event when the IMF B_z component was negative, and the B_x and B_Y components were the dominant components of the IMF.

[29] It is however possible that the observations of flow bursts poleward of the proton auroral spot may be related to an increase in the brightness of the proton auroral spot being associated with a lack of radar backscatter and possibly a deflection of ionospheric flow, with the increased plasma velocities observed in the region surrounding the enhanced auroral brightness. Ionospheric flow deflection has previously been observed by *Provan et al.* [2004] while performing a statistical study of high-latitude plasma flow during magnetospheric substorms. The flows were deflected around a region of suppressed flow, which was tentatively identified as the position of the auroral bulge. It was suggested that the flow stagnation and deflection could be due to the high electrical conductivity of the bulge ionosphere compared with the surrounding region [e.g., *Khan et al.*, 2001]. In the case study presented here there is no evidence of a flow suppression associated with the proton auroral spot, just a lack of radar backscatter. Further analysis is needed to determine whether this lack of radar backscatter could be related to enhanced particle precipitation and increased electrical conductivity associated with the proton spot.

[30] *Provan et al.* [2005] reported observing signatures of pulsed dayside reconnection both when simultaneous low-latitude and lobe merging was occurring and also when only lobe reconnection was observed. During the interval studied here we have observed solar wind pressure pulses with the quasiperiodic variation in the solar wind dynamic pressure directly correlated with fluctuations of the IMF B_z component, and found these pressure pulses to be directly correlated with fluctuations in the brightness of the auroral proton spot and with the high-latitude l-o-s velocities. *Frey et al.* [2002] observed the proton auroral spot when the IMF had a positive B_z component. They interpreted the proton spot as a direct signature of proton precipitation into the cusp after reconnection of magnetospheric lobe field lines. However, *Frey et al.* [2002] found that the intensity of the precipitation was not controlled by the magnitude of the IMF B_z component but rather by the solar wind dynamic pressure.

[31] For the interval presented in this study it has not been possible to confidently determine whether it is the solar wind pressure or the IMF B_z component, or both, which are modulating the auroral intensity, as these two parameters are significantly correlated with each other as well as with the fluctuations in the auroral intensity. However, it is worth noting that the correlation coefficient between the auroral brightness and the IMF B_z is ~0.6, which is clearly larger than the correlation coefficient between the auroral brightness and the solar wind pressure ($r \sim 0.43$). The pulsed nature of the ionospheric flow signatures demonstrate that the dayside reconnection rate is also being modulated. It is very interesting to note that the solar wind dynamic pressure

Figure 8. (a) Cross correlation between the proton auroral spot and ionospheric flow magnitude observed between 1600 and 1920 UT. Shown are peak brightness of the proton auroral spot (Figure 8a, top), average flow magnitude in the cusp region (Figure 8a, middle), and cross-correlation coefficient as a function of lag (Figure 8a, bottom). Two dashed lines overplotted on Figure 8a (bottom) indicate the correlation coefficient at which the two time series are correlated at a 99% significance level. (b) Correlation analysis between solar wind dynamic pressure and the IMF B_z component, presented in the same format as Figure 8a. (c) Correlation analysis between the solar wind dynamic pressure and the auroral brightness. (d) Correlation analysis between the IMF B_z component and auroral brightness. (e) Correlation analysis between the dayside ionospheric flow magnitude and the IMF B_z component. (f) Correlation analysis between the dayside ionospheric flow magnitude and the solar wind dynamic pressure.

has a periodicity of ~50 min, while the correlation coefficient between the auroral brightness and velocity magnitude also reaches a maximum at a lag of ~50 min. The intensity of the proton auroral spot has an average periodicity of ~22 min, almost half the periodicity of the of the solar wind dynamic pressure. This would suggest that the intensity of the proton auroral spot is positively correlated with both the maxima and minima in the solar wind dynamic pressure. However, although the correlation coefficient between the auroral brightness and solar wind dynamic pressure shows peaks at lag times of approximately −10 and approximately 27 min, these peaks were not found to be significant. Clearly, more work needs to be done in this area.

[32] We hypothesize that the dayside reconnection rate can be modulated both by variations in the IMF B_z component, and by changes in the solar wind dynamic pressure. Increases in the dynamic pressure would compress the magnetosphere and magnetotail and thus enhance the reconnection rate. This has previously been reported by *Farrugia et al.* [1995], who presented a case study of ground based optical observations for an interval when the IMF $B_z \sim 0$ and IMF $B_y \ll 0$. They observed auroral transients at the poleward edge of a latitudinally narrow zone of persistent auroral emission. They also observed a twin cell flow pattern with superimposed flow perturbations, and a sequence of magnetic impulses at ground stations around the optical sites which were correlated with the auroral transients. The authors found that the auroral transients were correlated with the arrival at the Earth of a sequence upstream solar wind pressure pulses. They interpreted their observations as being due to increases in the dynamic pressure at the dayside magnetopause which enhances the reconnection rate there. *Sandholt et al.* [1994] observed auroral transients and ground magnetic signatures of enhanced convection during an interval of negative IMF B_y and B_z. These transient signatures were also correlated with brief pulses in the solar wind dynamic pressure. However, enhancements in the auroral intensity can also be due to the enhancements in the plasma density resulting in increased precipitation of charged particles into the auroral region.

[33] This study leaves one crucial question unanswered: is dayside reconnection occurring at a weaker rate between these bursts of strong reconnection or does it stop entirely? Previous research by *Cowley and Lockwood* [1992] suggests that the flow excited by an impulsive reconnection event grows and decays with a timescale of the order of 10 min. The fact that the magnitude of the l-o-s velocity often increases by at least a factor of two during the flow bursts, indicates that the pulsations are very powerful. Thus it may well be that the weaker plasma flows observed between the flow pulsations, are driven by the strong flow bursts. Further research is needed to examine the timescale over which plasma flows and aurora excited by dayside reconnection decays below observable values.

5. Summary

[34] In this paper we have presented a case study concerning the proton auroral spot and conjugate ionospheric flows during one interval of prolonged northward IMF. During the first part of the interval the IMF B_y component dominated the B_z component and ionospheric flow patterns consistent with low-latitude merging occurring at the dayside magnetopause were observed. During the second part of the interval the IMF B_z component dominated the B_y component and we observed ionospheric flow patterns consistent with high-latitude lobe merging occurring. Throughout the interval we observed periodic fluctuations in the brightness of the proton auroral spot and correlated bursts of plasma flow. Simultaneously solar wind pressure pulses were observed, with fluctuations in the solar wind dynamic pressure correlated with variations in the IMF B_z component. The solar wind dynamic pressure and the IMF B_z component were both significantly correlated to the fluctuations in the plasma velocity and to the variations in the brightness of the proton auroral spot. The observations are consistent with the dayside reconnection rate and ionospheric precipitation being modulated by variations in the solar wind dynamic pressure and the IMF B_z component.

[35] **Acknowledgments.** We would like to thank the PIs of the SuperDARN radars for provision of the radar data employed in this study. The data employed were from radars funded by research funding agencies of Canada, France, Japan, the UK, and the USA. The CUTLASS radar is supported by the Particle Physics and Astronomy Research Council (PPARC grant PPA/R/R/1997/00256), U.K.; the Swedish Institute for Space Physics, Uppsala; and the Finnish Meteorological Institute, Helsinki. We would also like to thank Mike Ruohoniemi from John Hopkins University Applied Physics Laboratory for provision of the "Map Potential" algorithm software. For provision of the ACE magnetometer data we thank Norman Ness and Charles Smith of the Bartol Research Institute. We would like to thank Harald Frey at the Space Science Laboratory, University of Berkeley, for provision of the IMAGE SI-12 data. G.P. was supported during this study by PPARC grant PPA/G/O/2003/00013. S.W.H.C. was supported during this study by PPARC Senior Fellowship PPA/N/A/2000/00197. A.G. was supported during this study by PPARC grant PPA/G/0/2003/00013. During part of the preparation of the manuscript M.L. was supported by the Institute for Advanced Study, La Trobe University, Melbourne, Australia.

[36] Lou-Chuang Lee thanks Thomas Immel and Per Even Sandholt for their assistance in evaluating this manuscript.

References

Chisham, G., M. P. Freeman, I. J. Coleman, M. Pinnock, M. R. Hairston, M. Lester, and G. Sofko (2004), Measuring the dayside reconnection rate during an interval of due northward interplanetary magnetic field, *Ann. Geophys.*, *22*, 4243–4258.

Clauer, C. R., and E. Friis-Christensen (1988), High-latitude dayside electric fields and currents during strong northwards interplanetary magnetic field: Observation and model simulation, *J. Geophys. Res.*, *93*, 2749–2757.

Coumans, V., J. C. Gérard, B. Hubert, and D. S. Evans (2002), Electron and proton excitation of the FUV aurora: Simultaneous IMAGE and NOAA observations, *J. Geophys. Res.*, *107*(A11), 1347, doi:10.1029/2001JA009233.

Cowley, S. W. H., and M. Lockwood (1992), Excitation and decay of solar wind-driven flows in the magnetosphere-ionosphere system, *Ann. Geophys.*, *10*, 103–115.

Cowley, S. W. H., J. P. Morelli, and M. Lockwood (1991), Dependence of convective flows and particle-precipitation in the high-latitude dayside ionosphere on the x and y components of the interplanetary magnetic-field, *J. Geophys. Res.*, *96*, 5557–5564.

Farrugia, C. J., P. E. Sandholt, S. W. H. Cowley, D. J. Southwood, A. Egeland, P. Stauning, R. P. Lepping, A. J. Lazarus, T. Hansen, and E. Friis-Christensen (1995), Reconnection-associated auroral activity stimulated by two types of upstream dynamic pressure variations: Interplanetary magnetic field Bz ~ 0, By ≪ 0 case, *J. Geophys. Res.*, *100*, 21,753–21,772.

Farrugia, C. J., et al. (2004), Pulsed flows at the high-altitude cusp poleward boundary, and associated ionospheric convection and particle signatures, during a Cluster-FAST-SuperDARN-Sondrestrom conjunction under a southwest IMF, *Ann. Geophys.*, *22*, 2891–2905.

Freeman, M. P., C. J. Farrugia, M. R. Burlaga, L. F. Hairston, M. E. Greenspan, J. M. Ruohoniemi, and R. P. Lepping (1993), The interac-

tion of a magnetic cloud with the Earth: Ionospheric convection in the Northern and Southern hemispheres for a wide range of quasi-steady interplanetary magnetic conditions, *J. Geophys. Res.*, *98*, 7633–7656.
Frey, H. U., S. B. Mende, T. J. Immel, S. A. Fuselier, E. S. Claflin, J.-C. Gerard, and B. Hubert (2002), Proton aurora in the cusp, *J. Geophys. Res.*, *107*(A7), 1091, doi:10.1029/2001JA900161.
Frey, H. U., T. D. Phan, S. A. Fuselier, and S. B. Mende (2003a), Continuous magnetic reconnection at Earth's magnetopause, *Nature*, *426*, 533–537.
Frey, H. U., S. B. Mende, S. A. Fuselier, T. J. Immel, and N. Østgaard (2003b), Proton aurora in the cusp during southward IMF, *J. Geophys. Res.*, *108*(A7), 1277, doi:10.1029/2003JA009861.
Fuselier, S. A., H. U. Frey, K. J. Trattner, S. B. Mende, and J. L. Burch (2002), Cusp aurora dependence on interplanetary magnetic field B_z, *J. Geophys. Res.*, *107*(A7), 1111, doi:10.1029/2001JA900165.
Greenwald, R. A., et al. (1995a), Darn/SuperDARN: A global view of the dynamics of high-latitude convection, *Space Sci. Rev.*, *71*, 761–796.
Greenwald, R. A., W. A. Bristow, G. J. Sofko, C. Senior, J.-C. Cerisier, and A. Szabo (1995b), Super dual auroral radar network radar imaging of dayside high-latitude convection under northward interplanetary magnetic field: Toward resolving a distorted two-cell versus multicell controversy, *J. Geophys. Res.*, *100*, 19,661–19,674.
Heelis, R. A., P. H. Reiff, J. D. Winnigham, and W. B. Hanson (1986), Ionospheric convection signatures observed by DE2 during northward interplanetary magnetic field, *J. Geophys. Res.*, *91*, 5817–5830.
Huang, C.-S., D. A. Andre, G. J. Sofko, and A. V. Kustov (2000), Super Dual Auroral Radar Network observations of ionospheric multicell convection during northward interplanetary magnetic field, *J. Geophys. Res.*, *105*, 7419–7428.
Hubert, B., J.-C. Gérard, D. V. Bisikalo, D. V. Shematovich, and S. C. Solomon (2001), The role of proton precipitation in the excitation of auroral FUV emissions, *J. Geophys. Res.*, *106*, 21,475–21,494.
Khan, H., et al. (2001), Observations of two complete substorm cycles during the Cassini Earth swing-by: Cassini magnetometer data in a global context, *J. Geophys. Res.*, *106*, 30,141–30,175.
Knipp, D. J., A. D. Richmond, B. Emery, N. U. Crooker, O. de la Beaujardiere, D. Evans, and H. Kroehl (1991), Ionospheric convection response to changing IMF direction, *Geophys. Res. Lett.*, *18*, 721–724.
Lester, M., O. de la Beujardière, J. C. Foster, M. P. Freeman, H. Lühr, J. M. Ruohoniemi, and W. Swider (1993), The response of the large-scale ionospheric convection pattern to changes in the IMF and substorms: Results from the SUNDIAL 1987 campaign, *Ann. Geophys.*, *11*, 556–571.
McWilliams, K. A., T. K. Yeoman, and G. Provan (2000), A statistical survey of dayside pulsed ionospheric flows as seen by the CUTLASS Finland HF radar, *Ann. Geophys.*, *18*, 445–453.
Mende, S. B., et al. (2000a), Far ultraviolet imaging from the IMAGE spacecraft: 1. System design, *Space Sci. Rev.*, *91*, 243–270.
Mende, S. B., et al. (2000b), Far ultraviolet imaging from the IMAGE spacecraft: 3. Spectral imaging of Lyman alpha and OI 135.6 nm, *Space Sci. Rev.*, *91*, 287–318.
Milan, S. E., M. Lester, S. W. H. Cowley, and M. Brittnacher (2000a), Dayside convection and auroral morphology during an interval of northward interplanetary magnetic field, *Ann. Geophys.*, *18*, 436–444.
Milan, S. E., M. Lester, S. W. H. Cowley, and M. Brittnacher (2000b), Convection and auroral response to a southward turning of the IMF: POLAR UVI, CUTLASS and IMAGE signatures of transient magnetic flux transfer at the magnetopause, *J. Geophys. Res.*, *105*, 15,741–15,756.
Pinnock, M., A. S. Rodger, J. R. Dudeney, F. Rich, and K. B. Baker (1995), High spatial and temporal resolution observations of the ionospheric cusp, *Ann. Geophys.*, *13*, 919–925.
Provan, G., T. K. Yeoman, and S. E. Milan (1998), CUTLASS Finland Radar observations of the ionospheric signatures of flux transfer events and the resulting plasma flows, *Ann. Geophys.*, *16*, 1411–1422.
Provan, G., M. Lester, S. B. Mende, and S. E. Milan (2004), Statistical study of high-latitude plasma flow during magnetospheric substorms, *Ann. Geophys.*, *22*, 3607–3624.
Provan, G., M. Lester, A. Grocott, and S. W. H. Cowley (2005), Pulsed flows observed during an interval of prolonged northward IMF, *Ann. Geophys.*, *23*, 1207–1225.
Reiff, P. H., and J. L. Burch (1985), B_y-dependent dayside plasma flow and Birkeland currents in the dayside magnetosphere: 2. A global model for northward and southward IMF, *J. Geophys. Res.*, *90*, 1595–1609.
Rodger, A. S., and M. Pinnock (1997), The ionospheric response to flux transfer events: The first few minutes, *Ann. Geophys.*, *15*, 685–691.
Ruohoniemi, J. M., and K. B. Baker (1998), Large-scale imaging of high-latitude convection with Super Dual Auroral Radar Network HF radar observations, *J. Geophys. Res.*, *103*, 20,797–20,811.
Sandholt, P. E., J. Moen, D. Opsvik, W. F. Denig, and W. F. Burke (1993), Auroral event sequence at the dayside polar cap boundary: Signature of time-varying solar wind-magnetosphere-ionosphere coupling, *Adv. Space Res.*, *13*(4), 7–15.
Sandholt, P. E., et al. (1994), Cusp/cleft auroral activity in relation to solar wind dynamic pressure, interplanetary magnetic field B_z and B_y, *J. Geophys. Res.*, *99*, 17,323–17,343.
Sandholt, P. E., C. J. Farrugia, J. Moen, S. W. H. Cowley, and B. Lybekk (1998), Dynamics of the aurora and associated convection during a cusp bifurcation event, *Geophys. Res. Lett.*, *25*, 4313–4316.
Sandholt, P. E., C. J. Farrugia, S. W. H. Cowley, M. Lester, W. F. Denig, and J.-C. Cerisier (2000), Dynamic cusp aurora and associated pulsed reverse convection during northward IMF, *J. Geophys. Res.*, *105*, 12,869–12,894.
Smith, C. W., M. H. Acúna, L. F. Burlaga, J. L'Heureux, N. F. Ness, and J. Scheifele (1999), The ACE magnetic field experiment, *Space Sci. Rev.*, *86*, 613–632.
Thompson, S. M., M. G. Kivelson, K. K. Khurana, A. Balogh, H. Reme, A. N. Fazakerly, and L. M. Kistler (2004), Cluster observations of quasi-periodic impulsive signatures in the dayside northern lobe: High-latitude flux transfer events?, *J. Geophys. Res.*, *109*, A02213, doi:10.1029/2003JA010138.

S. W. H. Cowley, A. Grocott, M. Lester, S. E. Milan, and G. Provan, Department of Physics and Astronomy, University of Leicester, University Road, Leicester, LE1 7RH, UK. (gp3@ion.le.ac.uk)

B. Hubert, Laboratories de Physique Atmosphèrique et Planètaire, Université de Liège, Liège B-4000, Belgium.

H. Khan, Research and Scientific Support Department, SCI-SH Division, ESA/ESTEC, Keperlaan 1, Postbus 299, 2200 AG Noordwijk ZH, Netherlands.